Digital Comprehensive Summaries of Uppsala Dissertations
from the Faculty of Medicine 2023

Pitfalls in β-cell ion imaging with fluorescent indicators and their use for real-time detection of somatostatin secretion

MINGYU YANG

ACTA UNIVERSITATIS
UPSALIENSIS
2024

ISSN 1651-6206
ISBN 978-91-513-2048-9
urn:nbn:se:uu:diva-523019

UPPSALA
UNIVERSITET

Dissertation presented at Uppsala University to be publicly examined in B22, Biomedical Centre, Husargatan 3, Uppsala, Tuesday, 16 April 2024 at 09:15 for the degree of Doctor of Philosophy (Faculty of Medicine). The examination will be conducted in English. Faculty examiner: Docent Enming Zhang (Lund University, Department of Clinical Sciences).

Abstract
Yang, M. 2024. Pitfalls in β-cell ion imaging with fluorescent indicators and their use for real-time detection of somatostatin secretion. *Digital Comprehensive Summaries of Uppsala Dissertations from the Faculty of Medicine* 2023. 42 pp. Uppsala: Acta Universitatis Upsaliensis. ISBN 978-91-513-2048-9.

Fluorescent ion indicators have become indispensable tools in cell physiology. Dye indicators can easily be loaded into most types of cells, while genetically encoded indicators are advantageous in allowing specific cellular or subcellular targeting. Comparing responses of dye and protein-based indicators may provide useful insights into indicator properties and cellular processes. Here, a few genetically encoded Ca^{2+} indicators and fluorescent Ca^{2+} dyes were compared in insulin-secreting β-cells. Recordings of depolarization-triggered changes of the cytoplasmic Ca^{2+} concentration ($[Ca^{2+}]_i$) beneath the plasma membrane with total internal reflection fluorescence microscopy demonstrated distinct $[Ca^{2+}]_i$ spikes with protein-based indicators, while the dyes mainly reported stable $[Ca^{2+}]_i$ elevations. The spikes reflected Ca^{2+} release from the endoplasmic reticulum, triggered by autocrine purinergic receptor activation from exocytotic release of ATP. The indicator-dependent differences were unrelated to Ca^{2+} binding affinity and buffering and probably reflected slower Ca^{2+} dissociation kinetics of the protein indicators. In glucose-stimulated mouse islets, the dye Fura-2 reported the characteristic $[Ca^{2+}]_i$ response with an initial lowing followed by rapid increase, which was abolished by hyperpolarization with the K^+-channel opener diazoxide. The simultaneously present genetically encoded indicator R-GECO1 failed to detect the lowering and reported a spurious $[Ca^{2+}]_i$ elevation also in the presence of diazoxide, responses that could be ascribed to pH sensitivity of the indicator. Recordings with fluorescent H^+ indicators demonstrated that glucose increases cytoplasmic pH in β-cells. Elevations of $[Ca^{2+}]_i$ counteracted the alkalinization and $[Ca^{2+}]_i$ oscillations in glucose-stimulated islets were associated with anti-phasic oscillations of $[Ca^{2+}]_i$ and pH. A $[Ca^{2+}]_i$ imaging-based reporter cell assay for real-time detection of the islet hormone somatostatin was generated by transfecting HeLa cells with somatostatin receptor 2, the G-protein Gα15 and R-GECO1. The reporter cells detected somatostatin secretion from islets imaged in the same view-field as dose-dependent $[Ca^{2+}]_i$ elevations. Mouse and human islets released somatostatin in response to high K^+, glucose, and the hormones GLP-1 and ghrelin. In glucose-stimulated mouse islets, bursts of somatostatin release were synchronized with islet $[Ca^{2+}]_i$ oscillations. Analyses of islets from human donors indicated that type 2 diabetes is associated with hypersecretion of somatostatin. In conclusion, this thesis highlights potential pitfalls with fluorescent ion indicators in β-cell signalling studies and provides new insights into β-cell regulation of $[Ca^{2+}]_i$ and pH. Moreover, it introduces an assay for real-time detection of somatostatin secretion from islets that holds promise for studies of the role of this hormone under normal conditions and in diabetes.

Keywords: β-cells, cytoplasmic Ca^{2+}, cytoplasmic pH, fluorescent indicators, pancreatic islets, R-GECO1, somatostatin, type 2 diabetes

Mingyu Yang, Department of Medical Cell Biology, Box 571, Uppsala University, SE-75123 Uppsala, Sweden.

ISSN 1651-6206
ISBN 978-91-513-2048-9
URN urn:nbn:se:uu:diva-523019 (http://urn.kb.se/resolve?urn=urn:nbn:se:uu:diva-523019)

Till min familj och vänner

List of Papers

This thesis is based on the following papers, which are referred to in the text by their Roman numerals.

I. **Yang M,** Dyachok O, Xu Y, Gylfe E, Idevall-Hagren O, Tengholm A. (2023) Indicator-dependent differences in detection of local intracellular Ca^{2+} release events evoked by voltage-gated Ca^{2+} entry in pancreatic β-cells. *Cellular Signalling* 109:110805. doi: 10.1016/j.cellsig.2023.110805

II. **Yang M,** Dyachok O, Tengholm A. Detection of glucose-induced Ca^{2+} signals is perturbed by changes of cytoplasmic pH in β-cells. *Manuscript*.

III. **Yang M,** Mandal K, Dumral Ö, Winroth L, Tengholm A. Real-time detection of somatostatin release from single islets reveals hypersecretion in type 2 diabetes. *Submitted manuscript*.

Contents

Abbreviations

ADP	Adenosine diphosphate
ATP	Adenosine triphosphate
$[Ca^{2+}]_i$	Cytoplasmic Ca^{2+} concentration
cAMP	3',5'-cyclic adenosine monophosphate
CFP	Cyan fluorescent protein
ER	Endoplasmic reticulum
GPCR	G protein-coupled receptor
IP_3	Inositol 1,4,5-trisphosphate
K_{ATP} channel	ATP-sensitive K^+ channel
pH_i	Cytoplasmic pH
PLC	Phospholipase C
SERCA	Sarco/endoplasmic reticulum Ca^{2+}-ATPase
SSTR	Somatostatin receptor
TIRF	Total internal reflection fluorescence
VDCC	Voltage-dependent Ca^{2+} channels

Introduction

Pancreatic islets and diabetes

The islets of Langerhans in the pancreas release several hormones that are important for maintaining blood glucose homeostasis. Insulin is released from islet β-cells in response to increased blood glucose levels. Insulin promotes glucose storage in the liver and stimulates both uptake and storage of sugar in muscle and fat cells [1]. Glucagon is released from α-cells in response to lowering blood glucose concentrations with a main function to mobilize glucose from the liver [2]. A third hormone, somatostatin, is released from δ-cells and influences blood glucose indirectly by controlling the release of insulin and glucagon by paracrine effects on β- and α-cells [3, 4]. The release of the islet hormones is controlled by a multitude of regulating factors, including nutrients, other hormones, neurotransmitters as well as auto- and paracrine signals. The human pancreas contains 1-3 million islets [5] and that of rodents around 1000 islets [6]. The insulin-producing β-cells are most abundant and constitute approximately 50% of the cells in human islets and 75% in rodents. Glucagon-secreting α-cells constitute around 40% of the islet cells in humans and 15% in rodent islets, whereas only about 5% of the cells in both human and rodent islets are somatostatin-releasing δ-cells [7, 8]. In humans, the three types of cells are distributed throughout the islets, whereas in rodents, β-cells are located in the centre, surrounded by α- and δ-cells in the periphery [7-9]. Since δ-cells are elongated with filopodia-like structures, they can nevertheless make contact with many β- and α-cells within the islets [10]. β-cells are electrically coupled via gap junctions [11] and recent studies indicate such coupling also between β- and δ-cells [12], but there is also extensive auto- and paracrine signalling in the islets that control hormone secretion [13].

Failure of β-cells to secrete appropriate amounts of insulin leads to diabetes. There are two major types of diabetes: type 1, which is due to autoimmune β-cell destruction and type 2, which is caused by relative insulin deficiency, often in combination with insulin resistance. It has been estimated that 90-95% of all diabetes is type 2 diabetes [14]. Diabetes is often associated also with dysregulated glucagon secretion [15]. There is still limited understanding of the mechanisms underlying the defective release of the islet hormones in diabetes.

Ca^{2+} signalling in β-cells

Understanding the regulation of islet hormone secretion requires analyses of both intracellular signalling processes and hormone release. Many of the regulatory inputs result in a change in the cytoplasmic concentration of Ca^{2+} ($[Ca^{2+}]_i$), a ubiquitous second messenger, which, among other effects, triggers exocytosis of secretory granules [16, 17]. Like in most other cell types, the resting $[Ca^{2+}]_i$ in β-cells is at or below 100 nM. Influx of Ca^{2+} through voltage-dependent or other channels in the plasma membrane or release from the endoplasmic reticulum (ER) via inositol-1,4,5-trisphosphate (IP_3) receptors can trigger $[Ca^{2+}]_i$ increases reaching micromolar concentrations [18]. Glucose stimulates insulin secretion by increasing $[Ca^{2+}]_i$ in the β-cell. Glucose-stimulated β-cells in islets often show characteristic oscillations with both fast (2-5 min^{-1}) and slow (0.2-0.5 min^{-1}) frequency components [18]. The mechanism underlying glucose-induced $[Ca^{2+}]_i$ elevations involves entry of the sugar into the cell via glucose transporters (GLUT), followed by oxidative metabolism, leading to an increase in the cytoplasmic ATP/ADP ratio, which in turn results in closure of ATP-sensitive K^+ (K_{ATP}) channels, membrane depolarization and opening of voltage-dependent Ca^{2+} channels (VDCC). The glucose-induced increase in ATP/ADP ratio also stimulates uptake of Ca^{2+} into the ER by sarco/endoplasmic reticulum Ca^{2+}-ATPase (SERCA) [19, 20], preparing the cells to respond to agents acting via Gαq-protein coupled receptors and phospholipase C (PLC)-mediated generation of IP_3. One such agent is ATP, which is also present in the secretory granules and co-released with insulin. The release of ATP results in auto/paracrine activation of purinergic $P2Y_1$ receptors in the β-cell plasma membrane and IP_3-mediated Ca^{2+} release from the ER [21, 22]. Another example is acetylcholine, which is released from parasympathetic nerve endings [23] and as a paracrine signal from human α-cells [24]. Acetylcholine promotes Ca^{2+} mobilization in β-cells via muscarinic receptors [23]. The glucose-, ATP- and acetylcholine-induced Ca^{2+} signalling in β-cells is summarized in Figure 1.

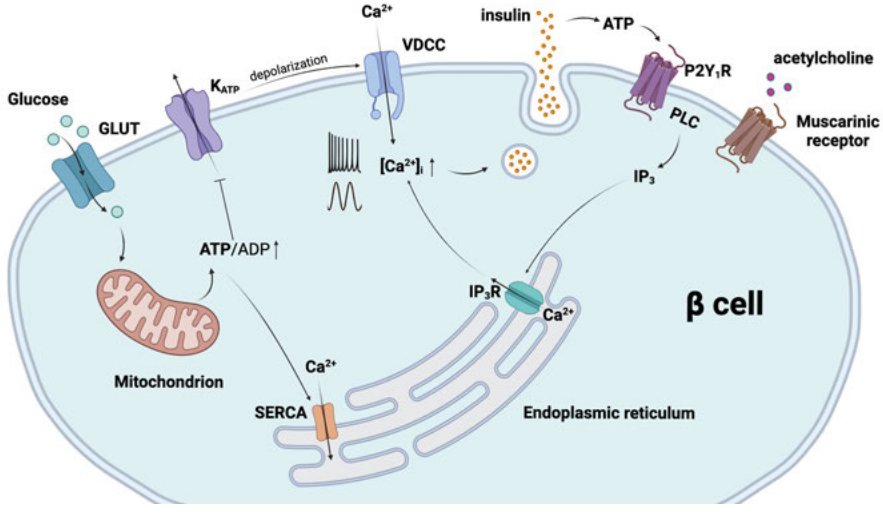

Figure 1. Ca^{2+} signalling in β-cells. See text for details.

Fluorescent Ca^{2+} indicators

Ca^{2+} signalling kinetics can be studied in living cells with fluorescent Ca^{2+} indicators. There are two principally different types of Ca^{2+} indicators: organic dyes and genetically encoded indicators, both with advantages and disadvantages. Fluorescent Ca^{2+} dyes, such as Fura-2, Fluo-5F and Fluo-4, have been used for several decades. The fluorescent dyes are quite convenient to use and can be easily loaded into most types of cells [25]. Typically, the charged carboxyl groups are shielded with acetoxymethyl esters to enhance lipophilicity and enable the dye to cross the plasma membrane. Inside the cell, the ester bonds are hydrolysed by non-specific esterases. The Ca^{2+}-binding carboxyl groups will then be exposed and the indicator becomes trapped in the cytoplasm [26]. Most of these fluorescent dyes have very high Ca^{2+} specificity, show limited cytotoxicity and are not very prone to photobleaching, features which make them suitable for monitoring Ca^{2+} dynamics in living cells [27, 28].

Genetically encoded fluorescent indicators (e.g., GCaMP5G and R-GECO1) have to be transfected into cells, but they instead have the advantage to be possible to target to specific subcellular localizations or populations of cells [28-31]. Most of the genetically encoded Ca^{2+} indicators are derived from calmodulin (CaM) and the M13 domain of the myosin light chain kinase in combination with various fluorescent proteins [31]. When Ca^{2+} binds to calmodulin, it will cause calmodulin and M13 domains to interact and the resulting conformational change can be read out either as altered fluorescence intensity of a circular

permuted fluorescent protein or as a change in Förster resonance energy transfer (FRET) between a pair of fluorescent proteins [32-34]. The protein-based indicators are increasingly used in different types of cells. Ca^{2+} signalling in β-cells has been extensively studied with fluorescent dyes but there is still limited experience with genetically encoded Ca^{2+} indicators, and side-by-side comparisons of the different classes of indicators have rarely been performed in physiologically relevant systems. Ca^{2+} indicators are often affected by pH [31, 35] and it may therefore be important to clarify if physiological pH changes affect the reported Ca^{2+} signal.

Cytoplasmic pH

Under physiological conditions, cytoplasmic pH (pH_i) is maintained at a value of 7.0 in most cells [36]. Several ion transporters are involved in regulating β-cell pH_i, such as the Na^+-H^+ exchanger (NHE) [37] and Na^+-HCO^- co-transporters (NBCs) [38, 39]. Organelles sometimes maintain a different pH than the cytoplasm [36, 40]. For example, ATP production in the mitochondria requires H^+ translocation [41]. With the H^+ extrusion, the mitochondria matrix is relatively alkaline (pH around 8). In contrast, organelles related to the endocytic and secretory pathways are typically acidic, such as lysosomes (pH ≈5), the Golgi apparatus (pH ≈6.5), and insulin granules (pH≈5-6). The low pH is suitable for many of the hydrolytic enzymes present in these organelles [36, 40, 42]. It has been suggested that the regulation of pH_i in β-cells affects insulin synthesis and secretion [43-45]. Glucose has been reported to induce alkalinization in pancreatic β-cells [37, 46, 47] but some studies also suggested that there is no effect [48] or acidification [49].

To investigate real-time pH_i changes in living cells, fluorescent pH indicators are suitable, as they have a high ion selectivity and allow imaging from single cells [50-52]. There are two types of pH indicators: fluorescent pH dyes, like BCECF, which has been widely used for decades [53]; and genetically encoded fluorescent pH indicators, which have been developed with the advent of fluorescent proteins technology [54].

Somatostatin and somatostatin receptors

Somatostatin was first found in and isolated from the hypothalamus in the early 1970s and was named from its action to inhibit the release of growth hormone in the pituitary [55, 56]. However, most (65%) of the total body somatostatin is produced in the gastrointestinal tract and only 5% originates from the pancreatic δ-cells [57]. There are two active isoforms of somatostatin, somatostatin 14 (SST-14) and somatostatin 28 (SST-28), both derived

from prosomatostatin. While SST-28 is mainly released from the gastrointestinal tract, SST-14 is dominating in the pancreatic δ-cells [58]. Somatostatin acts locally near its release site and the main function of islet somatostatin is to regulate insulin and glucagon secretion. Somatostatin exerts its effects through somatostatin receptors (SSTRs), of which there are five subtypes, SSTR1-5. All SSTRs are G protein-coupled receptors (GPCRs) mainly signalling via the Gαi protein, which among other downstream effects inhibits adenylyl cyclases (ACs) with resulting reduction of the intracellular cyclic adenosine 3'5'-monophosphate (cAMP) concentration ($[cAMP]_i$) [59]. The distribution and expression of SSTRs vary between different cell types. In human islets, SSTR2 shows high expression in both β- and α-cells [60, 61]. In the mouse, α-cells express mainly SSTR2, whereas SSTR3 seems to dominate in β-cells [62, 63].

Regulation of somatostatin secretion

Somatostatin secretion from islets is regulated by nutrients, including glucose, amino acids and fatty acids, as well as by hormones and neurotransmitters [64]. Many factors act directly on the δ-cells, but somatostatin release is also controlled by paracrine signalling from neighbouring β- and α-cells.

Glucose stimulates somatostatin release in both human and mouse islets and it is evident that somatostatin secretion is stimulated at glucose concentrations as low as 3 mM in mouse islets [65, 66]. The glucose-induced somatostatin secretion is complex and seems to involve several different mechanisms. Glucose causes the closure of K_{ATP} channels and Ca^{2+} entry via VDCC [67, 68]. The Ca^{2+} entry has been suggested to trigger Ca^{2+}-induced Ca^{2+} release from the ER [69]. Glucose-metabolism-generated ATP promotes this process by activating the SERCA pump and by stimulating cAMP formation, which facilitates Ca^{2+} release by a process that has been proposed to involve Epac interaction with ryanodine receptors [70]. Moreover, glucose transport into the δ-cell via sodium-dependent glucose cotransporter 2 (SGLT2) results in increased intracellular Na^+ concentration, which by a slight increase in $[Ca^{2+}]_i$ was suggested to trigger Ca^{2+}-induced Ca^{2+} release and thereby somatostatin release [71]. Glucose may also stimulate δ-cells indirectly via β-cells, since the cells are electrically coupled by gap junctions [12, 72]

Urocortin 3 is a 38-amino-acid peptide that belongs to the corticotropin-releasing factor family [73]. It has been suggested that urocortin 3 is co-released with insulin from β-cells [74] and that it activates the corticotropin releasing hormone receptor 2 (CRHR2) on δ-cells. CRHR2 in turn activates ACs and increases $[cAMP]_i$, which eventually leads to increased somatostatin secretion [75].

γ-Aminobutyric acid (GABA) is known as an inhibitory neurotransmitter, but is also released from β-cells and considered to trigger somatostatin release [76]. There are two main types of GABA receptors: ligand-gated Cl^- channels ($GABA_A$ receptors) and GPCRs ($GABA_B$ receptors). $GABA_A$ receptors are highly expressed in δ-cells, especially in human δ-cells [77]. Activation of these receptors induces membrane depolarization in β-cells and δ-cells, probably as a result of these cells being able to accumulate intracellular Cl^- beyond Nernst equilibrium. The depolarization in turn leads to Ca^{2+} influx through VDCC [76] and GABA can therefore be expected to stimulate somatostatin release.

Glucagon-like peptide-1 (GLP-1) receptors are highly expressed in β-cells and relatively highly in δ-cells compared to α-cells [78]. These receptors seem to be activated by both glucagon and GLP-1 [79, 80]. In both cases, there is Gαs-mediated activation of ACs with resulting stimulation of cAMP formation, which likely underlies the stimulation of somatostatin secretion [81].

Ghrelin is a peptide of 28 amino acids mainly produced in the stomach [82]. The peptide is also produced in islets from the rare ε-cells [83], and potentially also by other islets cell types [84]. In islets, the ghrelin receptor (GHSR), a GPCR that signals via Gαq, is selectively expressed in δ-cells and the hormone has consequently been found to stimulate somatostatin secretion [63]. Ghrelin is also known to inhibit insulin secretion, probably as a result of paracrine inhibition by somatostatin [62, 63, 84].

Glutamate is the major excitatory neurotransmitter. Pancreatic δ-cells express α-amino-3-hydroxy-5-methyl-4-isoxazolepropionic acid (AMPA) receptors, which belong to one of the ionotropic glutamate receptors (iGluR) families [85, 86]. Glutamate is therefore believed to induce δ-cell membrane depolarization and then increase $[Ca^{2+}]_i$ by opening VDCC and therefore stimulate somatostatin secretion [64]. Interestingly, at least in human islets, glutamate is co-released with glucagon from α-cells [87]. However, the role of glutamate in the regulation of somatostatin secretion is largely unknown.

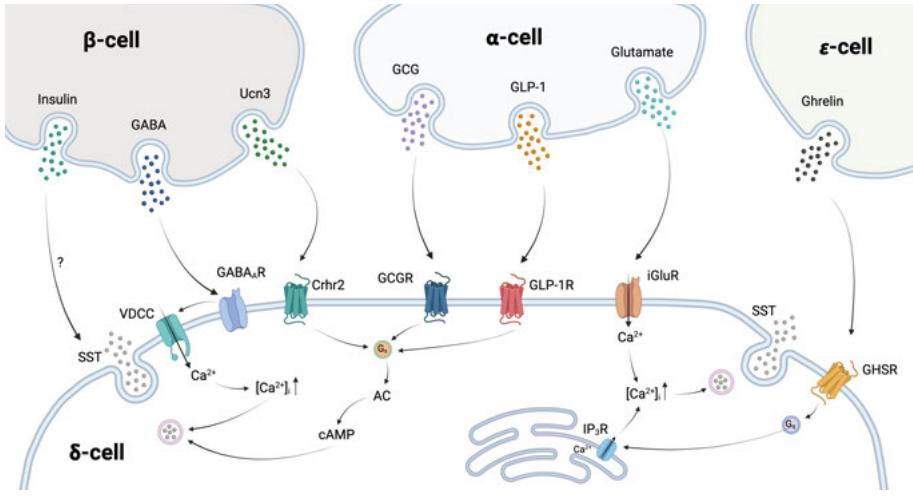

Figure 2. β- and α-cell-medicated paracrine regulation of δ-cells. See text for details.

Measurements of somatostatin release

Much less is known about the regulation of somatostatin release than about insulin and glucagon secretion. Shortage of δ-cells and difficulties in accessing them for physiological investigations have impeded development of the field. Measurements of somatostatin are mainly based on radioimmunoassay and enzyme-linked immunosorbent assay (ELISA) [88-91]. Both radioimmunoassays and ELISAs are specific but their sensitivities restrict studies of secretion to groups of islets and limited temporal resolution. Recently, an SSTR5-based sensor was developed to detect somatostatin release from isolated pancreatic islets [92]. This approach provides high spatial resolution information about somatostatin release, although it may not be a very efficient method for the determination of total release from the islets.

Aims

I. To clarify how depolarization-evoked $[Ca^{2+}]_i$ increases in β-cells are reported by fluorescent dyes and genetically encoded Ca^{2+} indicators.

II. To evaluate the ability of the genetically encoded Ca^{2+} indicator R-GECO1 to detect glucose-induced $[Ca^{2+}]_i$ signalling in β-cells and to determine the relationship between $[Ca^{2+}]_i$ and cytoplasmic pH.

III. To generate a Ca^{2+}-based optical reporter cell assay for real-time detection of somatostatin secretion from single islets.

Methodology

Insulin-secreting cells

The present studies employed the insulin-producing mouse β-cell line MIN6 as well as intact mouse and human islets. MIN6 cells originate from an insulinoma of a transgenic mouse expressing the SV40 T antigen in pancreatic β-cells [93]. The cells respond to physiological stimuli with insulin secretion similar to primary mouse β-cells. MIN6 cells were used in this study to characterize Ca^{2+} indicator properties in β-cells. In addition to constituting a pure β-cell preparation, MIN6 cells have the advantage of being easily transfected with plasmid vectors. The MIN6 cells were used between passages 20-32 and cultured in Dulbecco's Modified Eagle Medium (DMEM) with 25 mM glucose and supplemented with antibiotics, glutamine, mercaptoethanol and 15% FBS and then kept at 37°C in a humidified air atmosphere containing 5% CO_2.

Pancreatic islets

Although many features of β-cells can be studied in MIN6 cells, the cell line is insufficient for studying the physiology of β-cells within pancreatic islets with physical and paracrine interactions with other β-cells as well as with α- and δ-cells. In the present studies, both mouse and human islets were used. Mouse islets were isolated from 8-10 months old C57B16J mice (Scanbur, Sollentuna, Sweden). The pancreas was excised and placed in cold experimental buffer containing 138 mM NaCl, 4.8 mM KCl, 1.2 mM $MgCl_2$, 1.3 mM $CaCl_2$, 3 mM glucose and 25 mM HEPES with pH 7.40. The pancreas was then digested with 1.7 mg/ml collagenase P (Roche Dignostics, Solna, Stockholm) in a tissue shaker incubator and the digestion was terminated by addition of 0.1 g/ml bovine serum albumin (BSA). After washing, the islets were manually picked with a pipette and transferred to RPMI 1640 medium with 5.5 or 11 mM glucose and similar supplements as for DMEM but with 10 % FBS and without mercaptoethanol. The islets were cultured for 1-3 days at 37°C in an atmosphere with 5% CO_2. All animal experimental procedures were approved by the Uppsala Animal Ethics Committee.

Human islets were obtained from non-diabetic and type 2 diabetic (T2D) donors via the Nordic Network for Clinical Islet Transplantation in Uppsala.

Experimental handling was approved by Uppsala human ethics committee. Human islets were cultured in CMRL 1066 medium with 5.5 mM glucose and similar supplements as for RPMI 1640 medium for 3-5 days after delivery to laboratory.

HeLa cells

HeLa cells were used to generate reporter cells for somatostatin detection. This cell line originates from a human cervical carcinoma [94] and was chosen because the cells grow rapidly and are easy to culture and to transfect, and they are not excitatory and do not express SSTRs. HeLa cells were cultured in similar DMEM as described above (but without 2-mercaptoethanol and only 10% FBS).

Plasmid transfection and virus infection

To express genetically encoded Ca^{2+} sensors and/or SSTR2 in MIN6 or HeLa cells, the cells were transfected with a 100 µl OptiMEM medium mixture containing 0.2 µg plasmid DNA, 0.5 µl of Lipofectamine 2000 (Life technologies, Carlsbad, CA, USA). MIN6 cells (0.2 million cells per coverslip) or HeLa cells (50,000 cells per coverslip) were suspended in the mixture and added on to the centre of a 25-mm poly-L-lysine-coated coverslip. After transfection, 2 ml culture medium was added and cells were cultured in the incubator for at least 18 hours.

For gene transfer to primary cells, mouse and human islets were infected with adenoviruses containing the desired genetic constructs. A titre of 0.8 x 10^8 PFU/ml was used for R-GECO1 (Ca^{2+} indicator) and 1.2 x 10^9 PFU/ml for CFP-Venus (pH indicator). After 1.5-2 hours virus exposure the islets were washed twice with culture medium and further cultured overnight.

Fluorescence microscopy

To evaluate how Ca^{2+} indicators report depolarization-induced Ca^{2+} influx, most experiments were performed with total internal reflection fluorescence (TIRF) microscopy, which provides imaging in a narrow evanescent field reaching about 100 nm above the glass coverslip, and thus restricts the Ca^{2+} recording to cytoplasm immediately inside the plasma membrane. For imaging cells in a monolayer, a prism-based TIRF setup was used that was based on an E600FN upright microscope (Nikon) with a 16x, NA 0.8, water immersion objective. The excitation laser beam was homogenized using a rotating

light-shaping diffusor (Physical Optic Corp) and focused onto a modified quartz dove prism with 70˚ angle to achieve total internal reflection. For imaging of intact islets or islet cells, an objective-based TIRF setup was used. This imaging system used an inverted Eclipse Ti (Nikon) microscope with a 60x, NA 1.45, oil immersion objective. Both setups were equipped with diode-pumped solid-state lasers (Cobolt, Solna, Sweden) as source of excitation light. Band-pass filters (Semrock, IDEX Health & Science, LLC, Rochester, NY, USA) mounted in filter wheels (Sutter Instrument, Novato, CA, USA) were used for excitation and emission wavelength selection. Images were acquired with back-illuminated EMCCD cameras (DU-897, Andor Technology) controlled by MetaFluor software (Molecular Devices, Downingtown, PA, USA).

Global cytoplasmic Ca^{2+} and pH changes were measured with wide-field fluorescence microscopy using an Eclipse TE2000 microscope (Nikon) with a 40x objective (NA 1.3). Light emitting diodes (LedHUB, Omicron Laserage Laserprodukte GmbH, Rodgau, Germany) were used to provide excitation light. Emission wavelength was selected by filters in a wheel and images acquired with a MetaFluor-controlled EMCCD camera (DU-897 Andor Technology).

Confocal microscopy was used to image immunolabeled islets. An Eclipse Ti2 microscope (Nikon) was equipped with a Yokogawa CSU-X1A spinning disk confocal system (Visitron Systems GmbH), a 100x, NA 1.49 objective and a back-illuminated EMCCD camera (DU-888 Andor Technology). All devices were controlled with the MetaMorph software.

Ca^{2+} and pH imaging

In all imaging experiments, cells or islets were preincubated for 30-60 min in experimental buffer as described above. Cells and/or islets were allowed to attach to poly-L-lysine coated coverslips that were used as bottoms of a chamber with buffer superfusion of the cells.

To measure changes of the cytoplasmic Ca^{2+} concentration, both organic fluorescent Ca^{2+}dyes and genetically encoded Ca^{2+}indicators were used. The organic dyes Fluo-5F AM / Fluo-4 AM (Life technologies) / Cal-520 (AAT Bioquest, Sunnuvale, CA, USA) were used in most of the experiments in the paper I and III. The ratiometric Ca^{2+} dye Fura-2 LR (Ion Biosciences San Marcos, TX, USA) was used in some experiments in paper II. The ratiometric approach is advantageous in reducing the influence of some artifacts and therefore allows more reliable quantification of $[Ca^{2+}]_i$. To load the dye into cells or islets, the acetoxymethyl ester form of the dye was added to the preincubation buffer. The plasmids for the genetically encoded Ca^{2+}indicators R-GECO1 (Plasmid #45494) and GCaMP5G (Plasmid #31788) were obtained from Addgene (Watertown, MA, USA) and transfected into cells.

Adenoviruses for R-GECO1 and GCaMP5G were produced by Vector Biolabs (Philadelphia, PA, USA) and used for infection of pancreatic islets. The green fluorescent indicators Fluo-5F AM, Fluo-4 AM, Cal-520 and GCaMP5G were all excited at 491 nm and fluorescence was detected at 530/50 nm. The red fluorescent, protein-based Ca^{2+} indicator R-GECO1 was excited at 561 nm and its fluorescence was detected at >587 nm using a long-pass filter. For Fura-2 LR, the LED light source provided excitation at 340 and 380 nm and emission was measured at 510/40 nm.

For pH measurement, the ratiometric fluorescent pH dye BCFL was used in some experiments. However, the genetically encoded pH sensor CFP-Venus was used in most pH recordings because it showed a much better signal-to-noise ratio. Excitation of both CFP-Venus and BCFL was made with 427/10 nm and 504/12 nm LED light, while emission was detected at 475/42 nm and 538/40 nm. Cytoplasmic pH alterations were represented as the ratio of 504/427.

Fluorescence recovery after photobleaching (FRAP)

FRAP experiments were performed to investigate the mobility of the Ca^{2+} indicators by photobleaching a small region in MIN6 cells and determining the rate and fraction of fluorescence recovery. An objective-based TIRF system (Nikon 63x, NA 1.49) with galvomirror-based laser beam control (iLAS2, Gataca Systems, Massy, France) was used for imaging and photobleaching. A 3.5-µm diameter area within the Ca^{2+}-indicator-containing MIN6 cells was exposed to 405 nm laser light (Coherent Obis) with a 100-ms pulse to bleach the fluorophores and images were captured at 2 Hz to record the recovery kinetics.

Plasma membrane permeabilization

Some experiments were performed with permeabilized cells. By allowing control of the intracellular environment, permeabilized cells can be used to determine the Ca^{2+} sensitivity of different indicators. The MIN6 cells were permeabilized with 0.5 mg/ml α-toxin (PhPlate Stockholm, Stockholm, Sweden), in an intracellular-like buffer containing 6 mM NaCl, 140 mM KCl, 1 mM Mg-ATP, 2 mM EGTA, 2 mM HEDTA, 2 mM NTA and 10 mM HEPES and pH adjusted to 7.0. and after 15-20 mins, the toxin was washed away. The concentration of free Ca^{2+} was first maintained at 0.1 µM and subsequently increased stepwise to 300 µM.

Immunofluorescence staining

To investigate whether there is a correlation between the number of δ-cells and the amount of somatostatin secreted from pancreatic islets, human islets (from both non-diabetic or T2D donors) were collected after $[Ca^{2+}]_i$ imaging. The islets were first washed twice with PBS and this procedure was followed by 20 min fixation with paraformaldehyde and 5 min permeabilization with Triton X-100. Next, the primary antibodies against somatostatin (1:500, host: rabbit) and insulin (1:500, host: guinea pig, both from Dako, Sundbyberg, Sweden) were added into all islets and incubated for 2 h at room temperature. The islets were washed with PBS and then the secondary antibodies (anti-rabbit 647 nm, 1:500 and anti-guinea pig 488 nm, 1:500, both from Invitrogen, Göteborg, Sweden) were added for another 1 h incubation. Images of immunolabeled islets were acquired by confocal microscopy as described above.

Image analysis

Images from fluorescence microscopy were collected and analysed using MetaFluor software and data was analysed offline with Igor Pro software (Wavemetrics, Lake Oswego, OR).

Results and discussion

Sub-membrane imaging with genetically encoded Ca^{2+} indicators unmask depolarization-triggered $[Ca^{2+}]_i$ spikes in β-cells (Paper I)

Measuring the sub-membrane $[Ca^{2+}]_i$ responses to plasma membrane depolarization in β-cells with TIRF microscopy, it was noted that the genetically encoded Ca^{2+} indicators R-GECO1 and GCaMP5G frequently reported a different $[Ca^{2+}]_i$ response pattern than the fluorescent dye indicators Fluo-4 and Fluo-5F. In TIRF recordings of $[Ca^{2+}]_i$ from MIN6 cells depolarized with a high K^+ concentration, R-GECO1 and GCaMP5G often reported distinct $[Ca^{2+}]_i$ spikes from an elevated level, while Fluo-4 and Fluo-5F mainly reported stable $[Ca^{2+}]_i$ elevations. Depolarization of β-cells induces Ca^{2+} entry through voltage-dependent Ca^{2+} channels. However, the observed spikes were different from previously reported sub-membrane $[Ca^{2+}]_i$ spiking caused by voltage-gated Ca^{2+} influx [95]. Instead, it turned out that the spikes were secondary to exocytosis triggered by the depolarization-induced $[Ca^{2+}]_i$ elevation. During exocytosis, ATP is co-released with insulin and the nucleotide activates purinergic $P2Y_1$ receptors on the β-cell surface in an auto- and paracrine manner [22, 96], which in turn results in activation of PLC and IP_3-mediated release of Ca^{2+} from the ER [20, 23]. The $[Ca^{2+}]_i$ spikes now observed with R-GECO1 reflected such purinergic signalling, since they were abolished after depletion of ER Ca^{2+} by SERCA inhibition with cyclopiazonic acid as well as after inhibition of $P2Y_1$ receptors with the antagonist MRS2179. The β-cell spikes of $[Ca^{2+}]_i$ were also reported by the genetically encoded indicators when insulin secretion was stimulated by glucose. The appearance of $[Ca^{2+}]_i$ spikes were not restricted to MIN6 cells, but was also observed in primary β-cells in both mouse and human islets.

Indicator-dependent differences in $[Ca^{2+}]_i$ spike detection are unrelated to Ca^{2+} sensitivity, buffering and mobility (Paper I)

The difference in $[Ca^{2+}]_i$ spike detection between the indicators in TIRF microscopy may be caused by several factors, including Ca^{2+} binding affinity. The reported K_d value of R-GECO1 is 480 nM [31] which is similar to that of Fluo-4 (340 nM) [26], but much lower than the Fluo-5F K_d (2.3 μM) [97]. However, when the Ca^{2+} sensitivities were now investigated *in situ* by exposing permeabilized MIN6 cells to increasing Ca^{2+} concentrations in the nanomolar to micromolar range, the indicators showed similar and relatively low Ca^{2+} sensitivities with half-maximal fluorescence increases for R-GECO1, Fluo-4 and Fluo-5F at 3.0±0.3, 2.4±0.4 and 1.7±0.1 μM, respectively. Differences in Ca^{2+} binding affinity therefore cannot account for the observed difference in indicator responses.

Another factor that may influence detection of $[Ca^{2+}]_i$ spikes is that Ca^{2+} indicators exert a buffering effect. It is known that Ca^{2+} buffering may prevent detection of fast $[Ca^{2+}]_i$ changes [98]. The influence of buffering was now investigated by comparing the degree of spiking in cells loaded with low (0.3 μM) and high (3 μM) concentrations of the dye indicator acetoxymethyl esters. For both Fluo-4 and Fluo-5F, there was only a slight tendency towards increased number of spiking cells and higher amplitude of spikes at the lower loading concentration. When R-GECO1 and Fluo-5F were present in the same cell, $[Ca^{2+}]_i$ spikes were readily detected by R-GECO1, but not by Fluo-5F, providing evidence that Ca^{2+} buffering is not explaining the difference in $[Ca^{2+}]_i$ spike detection.

It may be envisaged that dye indicators with relatively small sizes are more diffusible in the cytoplasm and thereby more prone to "smear out" local changes in $[Ca^{2+}]_i$. The mobility of the indicators was therefore investigated by fluorescence recovery after photobleaching (FRAP) experiments. Although the mobile fraction of R-GECO1 was slightly higher than that of Fluo-4, FRAP analysis did not show major differences in recovery rate between R-GECO1 and Fluo-4, indicating that mobility is unlikely to explain the difference in detection of sub-membrane $[Ca^{2+}]_i$ spikes.

Slow Ca^{2+} dissociation kinetics may facilitate $[Ca^{2+}]_i$ spike detection in the sub-membrane compartment (Paper I)

Yet another potential explanation for the difference in $[Ca^{2+}]_i$ spike detection is related to the Ca^{2+} dissociation kinetics of the indicators. Since the spikes are caused by Ca^{2+} release from the ER, most of them can be expected to

originate from deeper parts of the cytoplasm than within the sub-membrane space monitored by TIRF microscopy. Indeed, when wide-field microscopy was applied to image the entire cytoplasm, both Fluo-5F and Fluo-4 reported significantly higher proportion of cells with $[Ca^{2+}]_i$ spikes than they did with TIRF microscopy. Among cells expressing R-GECO1, the fraction showing spikes was similar for the two imaging modes. The reason why protein indicators detect intracellular Ca^{2+} release events also in the sub-membrane space may be related to their markedly slower dissociation kinetics compared to the dye indicators. Calculated from reported k_{off} values and diffusion coefficients [31, 99-101], R-GECO1 would diffuse ≈30-fold longer than the dye indicators before Ca^{2+} dissociation. With a k_{off} of 0.752 s^{-1}, R-GECO1 would be able to diffuse a distance corresponding to the radius of a β-cell before releasing Ca^{2+} (≈6 µm assuming a diffusion coefficient of 20 $\mu m^2/s$ as for GFP [99]), whereas the dyes would only reach ≈0.4 µm (assuming a diffusion coefficient of 75 $\mu m^2/s$ as reported for Fluo-5F [101]). Accordingly, Ca^{2+}-bound protein indicators are more likely than Ca^{2+}-bound dyes to reach the sub-membrane space imaged with TIRF microscopy irrespective of where in the cell a Ca^{2+} release event takes place.

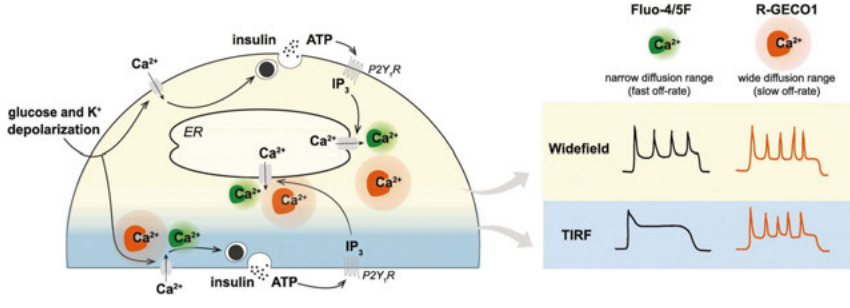

Figure 3. Slow Ca^{2+} dissociation kinetics may facilitate $[Ca^{2+}]_i$ spike detection in the sub-membrane compartment.

The observation that dye indicators rarely report $[Ca^{2+}]_i$ spikes in the sub-membrane compartment indicates that the exocytotic release of ATP from secretory granules does not trigger global purinergic signalling. It is more consistent with the view that the $P2Y_1$ receptors are activated close to the release site, resulting in restricted IP_3 formation and local ER Ca^{2+} release. This interpretation is supported by previous reports of local diacylglycerol domains in the plasma membrane following similar autocrine purinergic signalling [22]. Although the slow kinetics of the protein Ca^{2+} indicators in some situations may be considered advantageous in facilitating detection of $[Ca^{2+}]_i$ spikes, more recently developed versions modified for faster dissociation kinetics would be preferred for more faithful detection of local Ca^{2+} release events [102].

Glucose induces Ca^{2+}-independent changes in R-GECO1 fluorescence that coincide with alterations of pH_i (Paper II)

Continuing to characterize $[Ca^{2+}]_i$ signalling in β-cells with R-GECO1, mouse islets expressing the Ca^{2+} sensor were loaded with the classic ratiometric Ca^{2+} dye Fura-2 [103]. β-cells are known to respond to glucose stimulation with an initial $[Ca^{2+}]_i$ lowering that reflects SERCA-mediated uptake of Ca^{2+} into the ER energized by ATP formed in glucose metabolism [20]. The increased ATP/ADP ratio closes the K_{ATP} channels with concomitant membrane depolarization. When the glucose concentration was increased from 3 to 16.7 mM, Fura-2 reported the characteristic initial lowering of $[Ca^{2+}]_i$ [20] and the following $[Ca^{2+}]_i$ elevation with oscillations. In contrast to the initial lowering, R-GECO1 reported a small increase of fluorescence that was followed by further increase and oscillations coinciding with those detected with Fura-2. When the glucose concentration was restored to 3 mM, Fura-2 quickly reported a decrease to baseline $[Ca^{2+}]_i$, while R-GECO1 showed a delayed reduction preceded by a transient increase. One potential explanation for this difference is the Ca^{2+} sensitivity of the indicators. However, both R-GECO1 and Fura-2 similarly detected a small reduction in $[Ca^{2+}]_i$ caused by removing extracellular Ca^{2+} and modest elevation after depleting ER Ca^{2+} with SERCA blocker. The failure of R-GECO1 to detect the initial decrease induced by glucose stimulation was therefore not due to insufficient Ca^{2+} sensitivity. Interestingly, high glucose levels triggered an increase in R-GECO1 fluorescence within cells hyperpolarized with diazoxide, whereas Fura-2 detected the usual $[Ca^{2+}]_i$ decrease. When islets were restimulated with glucose in the absence of diazoxide, both R-GECO1 and Fura-2 reported $[Ca^{2+}]_i$ elevation. When diazoxide hyperpolarization was applied during glucose stimulation R-GECO1 fluorescence was only reduced by half whereas Fura-2 reported $[Ca^{2+}]_i$ reduction to baseline. These data indicate that glucose induces a Ca^{2+}-independent increase of R-GECO1 fluorescence.

R-GECO1 fluorescence is affected by its protonation state [104] and since glucose stimulation has been reported to trigger a rise in β-cell pH_i [37, 46, 47, 105], the Ca^{2+}-independent change in R-GECO1 signal may be related to altered pH_i. To test the effect of pH_i changes on the Ca^{2+} indicators, the genetically encoded ratiometric pH sensor (CFP-Venus) [106] was co-expressing with R-GECO1 in mouse islets and Fura-2 was subsequently loaded into the cells. When NH_4Cl was added to the medium, there was an immediate increase in pH_i and in R-GECO1 fluorescence, which seemed to be unrelated to Ca^{2+} since Fura-2 reported a slow and gradual $[Ca^{2+}]_i$ elevation. Elevation of the glucose concentration triggered alkalinization, which was detected by both CFP-Venus and the fluorescent pH dye BCFL. Similar glucose-induced increases in pH_i were also observed in hyperpolarized cells. The increase in pH

can be detected by R-GECO1 and misinterpreted as an increase in $[Ca^{2+}]_i$. The alkalinization commenced immediately after glucose stimulation, explaining why R-GECO1 failed to detect the initial $[Ca^{2+}]_i$ reduction. The mechanisms underlying glucose-induced pH changes in β-cells are still debated. Previous studies indicate that HCO_3^-/Cl^- exchangers and Na^+/H^+ exchangers are involved [37, 47, 105]. Overall, these findings indicate that the detection of glucose-induced Ca^{2+} signals by R-GECO1 is perturbed by pH_i changes in β-cells.

Synchronized $[Ca^{2+}]_i$ and pH_i oscillations in glucose-stimulated β-cells (Paper II)

Most β-cells respond to high glucose (16.7 mM) with characteristic $[Ca^{2+}]_i$ oscillations. In some cells, these oscillations were synchronized with oscillations in pH_i, with rises in $[Ca^{2+}]_i$ coinciding with reductions in pH_i. Preventing Ca^{2+} influx through hyperpolarization with diazoxide or voltage-gated Ca^{2+} channel inhibitor verapamil resulted in an increase in pH_i. These findings are in line with previous studies that Ca^{2+} acidifies the β-cell cytoplasm [47, 107]. In some cases when the voltage-dependent Ca^{2+} influx was inhibited, occasional transient $[Ca^{2+}]_i$ elevations were observed, which are known to reflect Ca^{2+} release from intracellular stores [21, 108], and also these transients were linked to slight reductions in pH_i. The exact reason behind Ca^{2+}-induced pH_i reduction remains unclear, but may involve several mechanisms. For example, interaction between Ca^{2+} and H^+ within Ca^{2+}-binding proteins, such as calmodulin [109]; Ca^{2+}-ATPases uses H^+ as counterion during Ca^{2+} transport [110]; and the ATP hydrolysis associated with Ca^{2+} transport results in production of a proton [111].

A reporter cell $[Ca^{2+}]_i$ signalling assay for somatostatin (Paper III)

Analysis of $[Ca^{2+}]_i$ may not only provide insights into the triggering signal for hormone release in islet cells. Activation of Gαq-coupled receptors triggers $[Ca^{2+}]_i$ elevation, and cells may be engineered to express a particular receptor, the activation of which can be detected by recordings of $[Ca^{2+}]_i$. Such cells can be used to detect release of hormones and other factors from islets [112]. To generate reporter cells for detection of somatostatin, SSTR2 was expressed in HeLa cells. Since this receptor is highly expressed in islet cells [62, 63], it should be suited to detect somatostatin released from δ-cells. Like other somatostatin receptors, SSTR2 inhibits ACs via Gαi but it has also been found to trigger PLC-dependent Ca^{2+} mobilization [113]. HeLa cells were therefore

transfected with SSTR2 alone or in combination with the G-protein Gα15, a member of the Gαq family, which links many receptors to PLC with resulting IP_3-mediated Ca^{2+} release from the ER [114, 115]. The cells were cotransfected with R-GECO1 for detection of Ca^{2+} specifically in the SSTR2-expressing cell population. Whereas control cells without SSTR2 did not show any $[Ca^{2+}]_i$ responses to high concentrations of somatostatin, HeLa cells with SSTR2 responded to somatostatin with dose-dependent $[Ca^{2+}]_i$ elevations. The sensitivity was higher for cells with both SSTR2 and Gα15 (EC_{50} 1.6±0.4 nM) compared to cells with SSTR2 alone (EC_{50} 9.8±0.9 nM) and the Gα15-SSTR2-expressing HeLa cells were therefore used in continued experiments aiming to detect release of endogenous somatostatin from pancreatic islets.

Detection of somatostatin secretion from mouse islets (Paper III)

To detect somatostatin release from mouse islets, the islets were first loaded with the green fluorescent Ca^{2+} dye Cal-520 and then placed onto a coverslip with previously plated reporter cells. The Ca^{2+} indicator enabled visualization of the islets in relation to the reporter cells and it enabled recording of $[Ca^{2+}]_i$ from the islets, although the focus was set to the reporter cells close to the coverslip. When the islets were depolarized by a high K^+ concentration (30 mM), there were robust $[Ca^{2+}]_i$ increases in both islets and reporter cells. The reporter cell response reflected somatostatin release, since it was inhibited by the SSTR2 antagonist CYN154806 and because control cells lacking SSTR2 did not respond to high K^+. Pancreatic δ-cells express K_{ATP} channels [63, 116]. Accordingly, δ-cell depolarization by closure of these channels with the sulfonylurea tolbutamide evoked somatostatin-dependent reporter cell $[Ca^{2+}]_i$ responses, but not to the same extent as K^+ depolarization. These experiments demonstrate that the reporter cell assay is capable of detecting depolarization-triggered somatostatin secretion from single mouse islets.

Glucose stimulation of somatostatin release (Paper III)

Glucose is a physiological stimulus for somatostatin release. Isolated mouse islets have been found to release somatostatin already in the presence of 3 mM glucose with half-maximal stimulation at 5-6 mM [66, 75, 117]. In line with such a high glucose sensitivity, some reporter cells now showed $[Ca^{2+}]_i$ signalling in the presence of mouse islets exposed to 1-3 mM glucose. Although there was no detectable $[Ca^{2+}]_i$ changes in the islets, the reporter cell responses indeed reflected somatostatin secretion and were consequently inhibited by SSTR2 blockade and by the K_{ATP} channel opener diazoxide, which

hyperpolarizes δ-cells. Increase of the glucose concentration to 7 and 11 mM triggered $[Ca^{2+}]_i$ elevation in the islets and was associated with increased $[Ca^{2+}]_i$ signalling in reporter cells, but there was no strong glucose concentration dependence of somatostatin secretion.

Glucose often induced characteristic slow and fast $[Ca^{2+}]_i$ oscillations in mouse islets [118-120]. These oscillations reflect the responses from β-cells, which are electrically coupled with gap junctions [121]. In some cases, the islet oscillations were clearly synchronized with $[Ca^{2+}]_i$ oscillations in the reporter cells, indicating that somatostatin is released in pulses that are coordinated with pulses of insulin driven by the synchronized $[Ca^{2+}]_i$ oscillations in β-cells. This observation is in line with previous studies demonstrating synchronous insulin and somatostatin pulsatility in the perfusate from human and mouse islets analysed with radioimmunoassay [72, 122]. It is also in line with the observation that $[Ca^{2+}]_i$ oscillations in glucose-stimulated β- and δ-cell are synchronized [123], an effect likely caused by electrical coupling between the two cell types [12].

Somatostatin secretion in response to neural, hormonal and intra-islet paracrine factors (Paper III)

Besides glucose, a number of neuro-hormonal and intra-islet paracrine factors have been reported to trigger somatostatin secretion. For example, insulin [124], glutamate [85], GABA [76] and urocortin 3 [74] have all been reported to stimulate somatostatin secretion. However, the reporter cells failed to respond when islets were exposed to these agents. In contrast, when islets were exposed to GLP-1 and ghrelin in the presence of 3 or 11 mM glucose, reporter cells responded with somatostatin-dependent $[Ca^{2+}]_i$ signalling. Glucagon was also an effective stimulator of somatostatin release, but only in the presence of 11 mM glucose. It is not clear whether the lack of effect of some agents is due to insufficient assay sensitivity, or whether the receptors for some of the factors were already activated by the concentrations present endogenously within the islets.

The effects of glucagon and GLP-1 are probably mediated via cAMP. It was sufficient to increase the cAMP concentration to trigger somatostatin secretion as both the AC activator forskolin and the phosphodiesterase inhibitor IBMX induced pronounced somatostatin-dependent $[Ca^{2+}]_i$ signalling in the reporter cells. This is in line with previous studies demonstrating that cAMP acts as a strong potentiator of somatostatin release [70]. It is important to note that none of the tested hormones, neurotransmitters or the cAMP-elevating agents had effects on reporter cell $[Ca^{2+}]_i$ in the absence of islets or on $[Ca^{2+}]_i$ in islet-associated control reporter cells lacking the SSTR2.

Detection of somatostatin secretion from human islets (Paper III)

Similar to mouse islets, human islets from non-diabetic organ donors induced somatostatin-dependent $[Ca^{2+}]_i$ increases in reporter cells when the glucose concentration was increased from 1 to 3, 7 and 11 mM. Glucagon, GLP-1 and ghrelin were also relatively strong stimuli of somatostatin release from human islets, while no effects were detected of glutamate, GABA, or urocortin 3. At variance with mouse islets, insulin triggered somatostatin secretion from human islets at 3 mM glucose in some donors.

Somatostatin secretion was also investigated in islets from human donors with type 2 diabetes. At 3 mM glucose, there was less $[Ca^{2+}]_i$ signalling in reporter cells with islets from diabetic compared to non-diabetic donors. Immunostaining of the islets collected after each experiment demonstrated that the diabetic donor islets contained fewer somatostatin-positive δ-cells, which supports a recent study [125]. However, when the islets were stimulated with high glucose or K^+, there was more pronounced $[Ca^{2+}]_i$ increases in reporter cells with the diabetic islets, indicating that somatostatin secretion may be increased under these conditions. Since the diabetic islets contained fewer δ-cells, increased somatostatin secretion must reflect a higher secretory activity in the remaining cells. Whether that reflects an inherent δ-cell phenomenon or if it is caused by other changes in the islets is not known. Increased somatostatin secretion during extended periods of time may potentially lead to down-regulation of somatostatin receptors in the islet. Interestingly, it was recently reported that α-cells from human type 2 diabetes donors showed less surface expression of somatostatin receptors and were relatively insensitive to inhibition from somatostatin [126].

Conclusions

Paper I

The different properties of synthetic Ca^{2+} dye and genetically encoded indicators may influence how $[Ca^{2+}]_i$ signals appear in TIRF and wide-field imaging modes. $[Ca^{2+}]_i$ signals in the sub-plasma-membrane compartment may reflect distant intracellular Ca^{2+} release events when protein indicators with slow dissociation kinetics are used. The use of different Ca^{2+} indicators may help to reveal important features of cell physiology. In β-cells, the strong link between voltage-dependent Ca^{2+} influx and Ca^{2+} release from the endoplasmic reticulum, often attributed to direct actions of Ca^{2+} on phospholipase C or intracellular release channels, seems to depend primarily on auto/paracrine purinergic signalling. The latter phenomenon has been underestimated with Ca^{2+} dyes.

Paper II

The study demonstrates that changes in pH_i caused by physiological glucose stimulation of β-cells distorts the signal from the red fluorescent Ca^{2+} indicator R-GECO1. Caution is therefore warranted when interpreting small changes in steady-state $[Ca^{2+}]_i$ and the indicator seems better suited for detection of distinct transient Ca^{2+} release events or pronounced Ca^{2+} influx. R-GECO1 thus does not faithfully report the glucose-induced initial lowering of $[Ca^{2+}]_i$ in β-cells because of the simultaneously occurring cytoplasmic alkalinization. These observations highlight the effect of glucose on pH_i in β-cells. Elevation of pH_i driven by glucose metabolism is counteracted by $[Ca^{2+}]_i$ elevations, which cause acidification and $[Ca^{2+}]_i$ oscillations in glucose-stimulated islets are therefore associated with pH_i oscillations in opposite phase. The significance of this phenomenon remains unknown but may have implications for many cellular processes.

Paper III

In this study, a $[Ca^{2+}]_i$ signalling-based reporter cell assay for semi-quantitative monitoring of somatostatin secretion was developed. The sensitivity allows real-time detection of somatostatin release from single islets. The study confirms previous observations that somatostatin secretion is stimulated by glucose and strongly enhanced by cAMP-elevating agents. Ghrelin was also found to be a robust stimulator of somatostatin release, but in contrast to the general view, this study did not find support for strong regulatory effects of glutamate, GABA, or urocortin 3. The results also indicate that somatostatin secretion is increased in islets from type 2 diabetic donors, a change that may lead to altered secretion of the other islet hormones.

Acknowledgement

My entire PhD study was undertaken at the Department of Medical Cell Biology, Uppsala University, Sweden. I would like to express my sincere gratitude to everyone I met during this journey.

First and foremost, great thanks to my supervisor *Anders Tengholm* for being my mentor since my master thesis project. Thanks for your unwavering support and patience throughout the entirety of this research journey. I appreciate all of our discussions whether science related or not. Your expertise, insightful feedback, and mentorship have been invaluable in shaping my research and helping me navigate the challenges of PhD study.

I am also indebted to my co-supervisors *Olof Idevall-Hagren* and *Sebastian Barg* for your insightful comments and suggestions during the various stages of my study, as well as your encouragement and willingness to provide assistance whenever needed.

To all my former and current group members in Idevall-Tengholm-Labs, thanks for making such an enjoyable working environment and always being supportive. I am pretty fortunate to have been in your company. It is amazing that, in this big and international group, we have not only become nice colleagues but also spent lots of time together as friends in life.

To all the colleagues in the department of MCB, thanks for creating a nice atmosphere and helping me deal with various problems even if it is irrelevant to science. It has been a pleasure to share all the different experiences with you, such as seminars for scientific discussion; interesting talks during lunchtime; food, fika and alcohol in the dining room and also those PhD days in the forest or hotel.

I extend my thanks to my friends outside the lab who are in Sweden, Bordeaux, Germany and China. Although we have limited opportunities to meet each other, especially during the pandemic, those times of having dinner, travelling and hangover together are very precious to me. It is with your company that makes my life more colourful and livelier.

Finally, I would like to express my heartfelt appreciation to my family.
感谢爸爸妈妈，是你们为这一切提供了可能。尽管距离和时差让我们的生活一直在发生着变化，但你们一直以来的爱与支持却从未改变，这也让我有了能够面对一切的底气。感谢所有的家人们，因为有你们，才让我无论何时回到家都能感受到家的温暖。

It is hard to imagine that it has been almost ten years since I came to Sweden in 2015. Along the way, I met many people who shared unforgettable memories. I appreciate all your kindness, help and support and you made it possible for me to complete this journey. Hope our paths cross again in the future!

谢谢! Tack! Thanks!

References

1. Saltiel, A.R. and C.R. Kahn, *Insulin signalling and the regulation of glucose and lipid metabolism.* Nature, 2001. **414**(6865): p. 799-806.
2. Jiang, G.Q. and B.B. Zhang, *Glucagon and regulation of glucose metabolism.* American Journal of Physiology-Endocrinology and Metabolism, 2003. **284**(4): p. E671-E678.
3. Bloom, S.R. and J.M. Polak, *Somatostatin.* Br Med J (Clin Res Ed), 1987. **295**(6593): p. 288-90.
4. Low, M.J., *Somatostatin.* Encyclopedia of Hormones, 2003.
5. Ionescu-Tirgoviste, C., et al., *A 3D map of the islet routes throughout the healthy human pancreas.* Sci Rep, 2015. **5**: p. 14634.
6. Alanentalo, T., et al., *Tomographic molecular imaging and 3D quantification within adult mouse organs.* Nat Methods, 2007. **4**(1): p. 31-3.
7. Brelje, T.C., D.W. Scharp, and R.L. Sorenson, *Three-dimensional imaging of intact isolated islets of Langerhans with confocal microscopy.* Diabetes, 1989. **38**(6): p. 808-14.
8. Brissova, M., et al., *Assessment of human pancreatic islet architecture and composition by laser scanning confocal microscopy.* J Histochem Cytochem, 2005. **53**(9): p. 1087-97.
9. Cabrera, O., et al., *The unique cytoarchitecture of human pancreatic islets has implications for islet cell function.* Proc Natl Acad Sci U S A, 2006. **103**(7): p. 2334-9.
10. Arrojo, E.D.R., et al., *Structural basis for delta cell paracrine regulation in pancreatic islets.* Nat Commun, 2019. **10**(1): p. 3700.
11. Theis, M., et al., *Replacement by a lacZ reporter gene assigns mouse connexin36, 45 and 43 to distinct cell types in pancreatic islets.* Exp Cell Res, 2004. **294**(1): p. 18-29.
12. Briant, L.J.B., et al., *delta-cells and beta-cells are electrically coupled and regulate alpha-cell activity via somatostatin.* J Physiol, 2018. **596**(2): p. 197-215.
13. Svendsen, B. and J.J. Holst, *Paracrine regulation of somatostatin secretion by insulin and glucagon in mouse pancreatic islets.* Diabetologia, 2021. **64**(1): p. 142-151.
14. American Diabetes, A., *2. Classification and Diagnosis of Diabetes: Standards of Medical Care in Diabetes-2020.* Diabetes Care, 2020. **43**(Suppl 1): p. S14-S31.
15. D'Alessio, D., *The role of dysregulated glucagon secretion in type 2 diabetes.* Diabetes Obes Metab, 2011. **13 Suppl 1**: p. 126-32.
16. Pang, Z.P. and T.C. Sudhof, *Cell biology of Ca2+-triggered exocytosis.* Curr Opin Cell Biol, 2010. **22**(4): p. 496-505.
17. Prentki, M., F.M. Matschinsky, and S.R. Madiraju, *Metabolic signaling in fuel-induced insulin secretion.* Cell Metab, 2013. **18**(2): p. 162-85.

18. Idevall-Hagren, O. and A. Tengholm, *Metabolic regulation of calcium signaling in beta cells.* Semin Cell Dev Biol, 2020. **103**: p. 20-30.
19. Roe, M.W., et al., *Thapsigargin inhibits the glucose-induced decrease of intracellular Ca2+ in mouse islets of Langerhans.* Am J Physiol, 1994. **266**(6 Pt 1): p. E852-62.
20. Chow, R.H., et al., *Coincidence of early glucose-induced depolarization with lowering of cytoplasmic Ca2+ in mouse pancreatic beta-cells.* J Physiol, 1995. **485 (Pt 3)**(Pt 3): p. 607-17.
21. Dyachok, O. and E. Gylfe, *Ca(2+)-induced Ca(2+) release via inositol 1,4,5-trisphosphate receptors is amplified by protein kinase A and triggers exocytosis in pancreatic beta-cells.* J Biol Chem, 2004. **279**(44): p. 45455-61.
22. Wuttke, A., O. Idevall-Hagren, and A. Tengholm, *P2Y(1) receptor-dependent diacylglycerol signaling microdomains in beta cells promote insulin secretion.* FASEB J, 2013. **27**(4): p. 1610-20.
23. Gilon, P. and J.C. Henquin, *Mechanisms and physiological significance of the cholinergic control of pancreatic beta-cell function.* Endocr Rev, 2001. **22**(5): p. 565-604.
24. Rodriguez-Diaz, R., et al., *Alpha cells secrete acetylcholine as a non-neuronal paracrine signal priming beta cell function in humans.* Nat Med, 2011. **17**(7): p. 888-92.
25. Thomas, D., et al., *A comparison of fluorescent Ca2+ indicator properties and their use in measuring elementary and global Ca2+ signals.* Cell Calcium, 2000. **28**(4): p. 213-23.
26. Gee, K.R., et al., *Chemical and physiological characterization of fluo-4 Ca(2+)-indicator dyes.* Cell Calcium, 2000. **27**(2): p. 97-106.
27. Rietdorf, K., et al., *Novel improved Ca 2+ indicator dyes on the market-a comparative study of novel Ca 2+ indicators with fluo-4.* 2014.
28. Lock, J.T., I. Parker, and I.F. Smith, *A comparison of fluorescent Ca(2)(+) indicators for imaging local Ca(2)(+) signals in cultured cells.* Cell Calcium, 2015. **58**(6): p. 638-48.
29. Tsien, R.Y., *The green fluorescent protein.* Annu Rev Biochem, 1998. **67**: p. 509-44.
30. Nakai, J., M. Ohkura, and K. Imoto, *A high signal-to-noise Ca(2+) probe composed of a single green fluorescent protein.* Nat Biotechnol, 2001. **19**(2): p. 137-41.
31. Zhao, Y., et al., *An expanded palette of genetically encoded Ca(2)(+) indicators.* Science, 2011. **333**(6051): p. 1888-91.
32. Miyawaki, A., et al., *Fluorescent indicators for Ca2+ based on green fluorescent proteins and calmodulin.* Nature, 1997. **388**(6645): p. 882-7.
33. Wang, Q., et al., *Structural basis for calcium sensing by GCaMP2.* Structure, 2008. **16**(12): p. 1817-27.
34. Akerboom, J., et al., *Crystal structures of the GCaMP calcium sensor reveal the mechanism of fluorescence signal change and aid rational design.* J Biol Chem, 2009. **284**(10): p. 6455-64.
35. Russell, J.T., *Imaging calcium signals in vivo: a powerful tool in physiology and pharmacology.* Br J Pharmacol, 2011. **163**(8): p. 1605-25.
36. Putnam, R. and N. Sperelakis, *Cell Physiology Source Book.* 2012.
37. Stiernet, P., et al., *Glucose-induced cytosolic pH changes in beta-cells and insulin secretion are not causally related: studies in islets lacking the Na+/H+ exchangeR NHE1.* J Biol Chem, 2007. **282**(34): p. 24538-46.
38. Wang, Y.J., et al., *Single-Cell Transcriptomics of the Human Endocrine Pancreas.* Diabetes, 2016. **65**(10): p. 3028-38.

39. Brown, M.R., et al., *Electrogenic sodium bicarbonate cotransporter NBCe1 regulates pancreatic beta cell function in type 2 diabetes.* J Clin Invest, 2021. **131**(17).
40. Casey, J.R., S. Grinstein, and J. Orlowski, *Sensors and regulators of intracellular pH.* Nat Rev Mol Cell Biol, 2010. **11**(1): p. 50-61.
41. Papa, S., et al., *Proton translocation and energy transduction in mitochondria.* Biochimie, 1973. **55**(6): p. 703-16.
42. Paroutis, P., N. Touret, and S. Grinstein, *The pH of the secretory pathway: measurement, determinants, and regulation.* Physiology (Bethesda), 2004. **19**: p. 207-15.
43. Hutton, J.C., *The internal pH and membrane potential of the insulin-secretory granule.* Biochem J, 1982. **204**(1): p. 171-8.
44. Pace, C.S., J.T. Tarvin, and J.S. Smith, *Stimulus-secretion coupling in beta-cells: modulation by pH.* Am J Physiol, 1983. **244**(1): p. E3-18.
45. Gunawardana, S.C., et al., *Nutrient-stimulated insulin secretion in mouse islets is critically dependent on intracellular pH.* BMC Endocr Disord, 2004. **4**(1): p. 1.
46. Lindstrom, P. and J. Sehlin, *Effect of glucose on the intracellular pH of pancreatic islet cells.* Biochem J, 1984. **218**(3): p. 887-92.
47. Shepherd, R.M. and J.C. Henquin, *The role of metabolism, cytoplasmic Ca2+, and pH-regulating exchangers in glucose-induced rise of cytoplasmic pH in normal mouse pancreatic islets.* J Biol Chem, 1995. **270**(14): p. 7915-21.
48. Grapengiesser, E., E. Gylfe, and B. Hellman, *Regulation of pH in individual pancreatic beta-cells as evaluated by fluorescence ratio microscopy.* Biochim Biophys Acta, 1989. **1014**(3): p. 219-24.
49. Pace, C.S. and J.T. Tarvin, *Amiloride-sensitive regulation of intracellular pH in B-cells: activation by glucose.* Metabolism, 1986. **35**(2): p. 176-81.
50. Boyer, M.J. and D.W. Hedley, *Measurement of intracellular pH.* Methods Cell Biol, 1994. **41**: p. 135-48.
51. Loiselle, F.B. and J.R. Casey, *Measurement of Intracellular pH.* Methods Mol Biol, 2010. **637**: p. 311-31.
52. Han, J. and K. Burgess, *Fluorescent indicators for intracellular pH.* Chem Rev, 2010. **110**(5): p. 2709-28.
53. Rink, T.J., R.Y. Tsien, and T. Pozzan, *Cytoplasmic pH and free Mg2+ in lymphocytes.* J Cell Biol, 1982. **95**(1): p. 189-96.
54. Martynov, V.I., et al., *Genetically encoded fluorescent indicators for live cell pH imaging.* Biochim Biophys Acta Gen Subj, 2018. **1862**(12): p. 2924-2939.
55. Krulich, L., Dhariwal, A. P. S., and McCann, S. M. , *Stimulatory and Inhibitory Effects of Purified Hypothalamic Extracts on Growth Hormone Release from Rat Pituitary in Vitro.* Endocrinology, 1968. **83**(4): p. 783-790.
56. Brazeau, P., et al., *Hypothalamic polypeptide that inhibits the secretion of immunoreactive pituitary growth hormone.* Science, 1973. **179**(4068): p. 77-9.
57. Martinez, V.T., Y., *Somatostatin In: Johnson L (ed) Encyclopedia of Gastroenterology, 1st ed.*, in *Elsevier*. 2004. p. pp 426–433.
58. Francis, B.H., et al., *Distribution of somatostatin-14 and somatostatin-28 gastrointestinal-pancreatic cells of rats and humans.* Gastroenterology, 1990. **99**(5): p. 1283-91.
59. Patel, Y.C. and C.B. Srikant, *Somatostatin receptors.* Trends Endocrinol Metab, 1997. **8**(10): p. 398-405.
60. Barnett, P., *Somatostatin and somatostatin receptor physiology.* Endocrine, 2003. **20**(3): p. 255-64.

61. Kailey, B., et al., *SSTR2 is the functionally dominant somatostatin receptor in human pancreatic beta- and alpha-cells.* Am J Physiol Endocrinol Metab, 2012. **303**(9): p. E1107-16.
62. Adriaenssens, A.E., et al., *Transcriptomic profiling of pancreatic alpha, beta and delta cell populations identifies delta cells as a principal target for ghrelin in mouse islets.* Diabetologia, 2016. **59**(10): p. 2156-65.
63. DiGruccio, M.R., et al., *Comprehensive alpha, beta and delta cell transcriptomes reveal that ghrelin selectively activates delta cells and promotes somatostatin release from pancreatic islets.* Mol Metab, 2016. **5**(7): p. 449-458.
64. Gao, R., T. Yang, and Q. Zhang, *delta-Cells: The Neighborhood Watch in the Islet Community.* Biology-Basel, 2021. **10**(2).
65. Berts, A., et al., *Glucose stimulation of somatostatin-producing islet cells involves oscillatory Ca2+ signaling.* Endocrinology, 1996. **137**(2): p. 693-7.
66. Vieira, E., A. Salehi, and E. Gylfe, *Glucose inhibits glucagon secretion by a direct effect on mouse pancreatic alpha cells.* Diabetologia, 2007. **50**(2): p. 370-9.
67. Gopel, S.O., et al., *Patch-clamp characterisation of somatostatin-secreting -cells in intact mouse pancreatic islets.* J Physiol, 2000. **528**(Pt 3): p. 497-507.
68. Hauge-Evans, A.C., et al., *Somatostatin secreted by islet delta-cells fulfills multiple roles as a paracrine regulator of islet function.* Diabetes, 2009. **58**(2): p. 403-11.
69. Zhang, Q., et al., *R-type Ca(2+)-channel-evoked CICR regulates glucose-induced somatostatin secretion.* Nat Cell Biol, 2007. **9**(4): p. 453-60.
70. Denwood, G., et al., *Glucose stimulates somatostatin secretion in pancreatic delta-cells by cAMP-dependent intracellular Ca(2+) release.* J Gen Physiol, 2019. **151**(9): p. 1094-1115.
71. Vergari, E., et al., *Somatostatin secretion by Na(+)-dependent Ca(2+)-induced Ca(2+) release in pancreatic delta-cells.* Nat Metab, 2020. **2**(1): p. 32-40.
72. Hellman, B., et al., *Glucose generates coincident insulin and somatostatin pulses and antisynchronous glucagon pulses from human pancreatic islets.* Endocrinology, 2009. **150**(12): p. 5334-40.
73. Lewis, K., et al., *Identification of urocortin III, an additional member of the corticotropin-releasing factor (CRF) family with high affinity for the CRF2 receptor.* Proceedings of the National Academy of Sciences of the United States of America, 2001. **98**(13): p. 7570-7575.
74. van der Meulen, T., et al., *Urocortin3 mediates somatostatin-dependent negative feedback control of insulin secretion.* Nat Med, 2015. **21**(7): p. 769-76.
75. Rorsman, P. and M.O. Huising, *The somatostatin-secreting pancreatic delta-cell in health and disease.* Nat Rev Endocrinol, 2018. **14**(7): p. 404-414.
76. Braun, M., et al., *gamma-Aminobutyric Acid (GABA) Is an Autocrine Excitatory Transmitter in Human Pancreatic beta-Cells.* Diabetes, 2010. **59**(7): p. 1694-1701.
77. Korol, S.V., et al., *Functional Characterization of Native, High-Affinity GABA(A) Receptors in Human Pancreatic beta Cells.* EBioMedicine, 2018. **30**: p. 273-282.
78. Richards, P., et al., *Identification and characterization of GLP-1 receptor-expressing cells using a new transgenic mouse model.* Diabetes, 2014. **63**(4): p. 1224-33.
79. Holst, J.J., *The physiology of glucagon-like peptide 1.* Physiological Reviews, 2007. **87**(4): p. 1409-1439.

80. Shuai, H., et al., *Glucose-induced cAMP elevation in beta-cells involves amplification of constitutive and glucagon-activated GLP-1 receptor signalling.* Acta Physiol (Oxf), 2021. **231**(4): p. e13611.
81. Gromada, J., J.J. Holst, and P. Rorsman, *Cellular regulation of islet hormone secretion by the incretin hormone glucagon-like peptide 1.* Pflugers Archiv-European Journal of Physiology, 1998. **435**(5): p. 583-594.
82. Kojima, M., et al., *Ghrelin is a growth-hormone-releasing acylated peptide from stomach.* Nature, 1999. **402**(6762): p. 656-60.
83. Wierup, N., et al., *The ghrelin cell: a novel developmentally regulated islet cell in the human pancreas.* Regul Pept, 2002. **107**(1-3): p. 63-9.
84. Dezaki, K. and T. Yada, *Status of ghrelin as an islet hormone and paracrine/autocrine regulator of insulin secretion.* Peptides, 2022. **148**: p. 170681.
85. Muroyama, A., et al., *A novel variant of ionotropic glutamate receptor regulates somatostatin secretion from delta-cells of islets of Langerhans.* Diabetes, 2004. **53**(7): p. 1743-53.
86. Traynelis, S.F., et al., *Glutamate Receptor Ion Channels: Structure, Regulation, and Function.* Pharmacological Reviews, 2010. **62**(3): p. 405-496.
87. Takahashi, H., N. Yokoi, and S. Seino, *Glutamate as intracellular and extracellular signals in pancreatic islet functions.* Proceedings of the Japan Academy Series B-Physical and Biological Sciences, 2019. **95**(6): p. 246-260.
88. Grange, R.D., J.P. Thompson, and D.G. Lambert, *Radioimmunoassay, enzyme and non-enzyme-based immunoassays.* Br J Anaesth, 2014. **112**(2): p. 213-6.
89. Vonen, B., et al., *Radio-immunoassay of somatostatin from isolated rat pancreatic islets.* Scand J Clin Lab Invest, 1989. **49**(2): p. 135-8.
90. Yalow, R.S. and S.A. Berson, *Assay of plasma insulin in human subjects by immunological methods.* Nature, 1959. **184 (Suppl 21)**: p. 1648-9.
91. Engvall, E. and P. Perlmann, *Enzyme-linked immunosorbent assay (ELISA). Quantitative assay of immunoglobulin G.* Immunochemistry, 1971. **8**(9): p. 871-4.
92. Wang, H., et al., *A tool kit of highly selective and sensitive genetically encoded neuropeptide sensors.* Science, 2023. **382**(6672): p. eabq8173.
93. Miyazaki, J., et al., *Establishment of a pancreatic beta cell line that retains glucose-inducible insulin secretion: special reference to expression of glucose transporter isoforms.* Endocrinology, 1990. **127**(1): p. 126-32.
94. Landry, J.J., et al., *The genomic and transcriptomic landscape of a HeLa cell line.* G3 (Bethesda), 2013. **3**(8): p. 1213-24.
95. Langlhofer, G., A. Kogel, and M. Schaefer, *Glucose-induced [Ca2+]i oscillations in beta cells are composed of trains of spikes within a subplasmalemmal microdomain.* Cell Calcium, 2021. **99**: p. 102469.
96. Khan, S., et al., *Autocrine activation of P2Y1 receptors couples Ca (2+) influx to Ca (2+) release in human pancreatic beta cells.* Diabetologia, 2014. **57**(12): p. 2535-45.
97. Matthews, H.R. and G.L. Fain, *A light-dependent increase in free Ca2+ concentration in the salamander rod outer segment.* J Physiol, 2001. **532**(Pt 2): p. 305-21.
98. Dyachok, O., G. Tufveson, and E. Gylfe, *Ca2+-induced Ca2+ release by activation of inositol 1,4,5-trisphosphate receptors in primary pancreatic beta-cells.* Cell Calcium, 2004. **36**(1): p. 1-9.
99. Potma, E.O., et al., *Reduced protein diffusion rate by cytoskeleton in vegetative and polarized dictyostelium cells.* Biophys J, 2001. **81**(4): p. 2010-9.

100. Delvendahl, I., et al., *Reduced endogenous Ca2+ buffering speeds active zone Ca2+ signaling.* Proc Natl Acad Sci U S A, 2015. **112**(23): p. E3075-84.
101. Hamid, E., E. Church, and S. Alford, *Quantitation and Simulation of Single Action Potential-Evoked Ca(2+) Signals in CA1 Pyramidal Neuron Presynaptic Terminals.* eNeuro, 2019. **6**(5).
102. Kerruth, S., et al., *The kinetic mechanisms of fast-decay red-fluorescent genetically encoded calcium indicators.* J Biol Chem, 2019. **294**(11): p. 3934-3946.
103. Grynkiewicz, G., M. Poenie, and R.Y. Tsien, *A new generation of Ca2+ indicators with greatly improved fluorescence properties.* J Biol Chem, 1985. **260**(6): p. 3440-50.
104. Molina, R.S., et al., *Understanding the Fluorescence Change in Red Genetically Encoded Calcium Ion Indicators.* Biophys J, 2019. **116**(10): p. 1873-1886.
105. Juntti-Berggren, L., et al., *Glucose-induced increase in cytoplasmic pH in pancreatic beta-cells is mediated by Na+/H+ exchange, an effect not dependent on protein kinase C.* J Biol Chem, 1991. **266**(35): p. 23537-41.
106. Su, S., et al., *Genetically encoded calcium indicator illuminates calcium dynamics in primary cilia.* Nat Methods, 2013. **10**(11): p. 1105-7.
107. Salgado, A., et al., *Multiphasic action of glucose and alpha-ketoisocaproic acid on the cytosolic pH of pancreatic beta-cells. Evidence for an acidification pathway linked to the stimulation of Ca2+ influx.* J Biol Chem, 1996. **271**(15): p. 8738-46.
108. Thore, S., et al., *Feedback activation of phospholipase C via intracellular mobilization and store-operated influx of Ca2+ in insulin-secreting beta-cells.* J Cell Sci, 2005. **118**(Pt 19): p. 4463-71.
109. Busa, W.B. and R. Nuccitelli, *Metabolic regulation via intracellular pH.* Am J Physiol, 1984. **246**(4 Pt 2): p. R409-38.
110. Daugirdas, J.T., et al., *Intracellular acidification associated with changes in free cytosolic calcium. Evidence for Ca2+/H+ exchange via a plasma membrane Ca(2+)-ATPase in vascular smooth muscle cells.* J Clin Invest, 1995. **95**(4): p. 1480-9.
111. Silverstein, T.P., *The Proton in Biochemistry: Impacts on Bioenergetics, Biophysical Chemistry, and Bioorganic Chemistry.* Front Mol Biosci, 2021. **8**: p. 764099.
112. Cabrera, O., et al., *Glutamate is a positive autocrine signal for glucagon release.* Cell Metab, 2008. **7**(6): p. 545-54.
113. Tomura, H., et al., *Transfected human somatostatin receptor type 2, SSTR2, not only inhibits adenylate cyclase but also stimulates phospholipase C and Ca2+ mobilization.* Biochem Biophys Res Commun, 1994. **200**(2): p. 986-92.
114. Wilkie, T.M., et al., *Evolution of the mammalian G protein alpha subunit multigene family.* Nat Genet, 1992. **1**(2): p. 85-91.
115. Offermanns, S. and M.I. Simon, *G alpha 15 and G alpha 16 couple a wide variety of receptors to phospholipase C.* J Biol Chem, 1995. **270**(25): p. 15175-80.
116. Braun, M., et al., *Somatostatin release, electrical activity, membrane currents and exocytosis in human pancreatic delta cells.* Diabetologia, 2009. **52**(8): p. 1566-78.
117. Walker, J.N., et al., *Regulation of glucagon secretion by glucose: paracrine, intrinsic or both?* Diabetes Obes Metab, 2011. **13 Suppl 1**: p. 95-105.

118. Bergsten, P., et al., *Synchronous oscillations of cytoplasmic Ca2+ and insulin release in glucose-stimulated pancreatic islets.* J Biol Chem, 1994. **269**(12): p. 8749-53.
119. Liu, Y.J., et al., *Origin of slow and fast oscillations of Ca2+ in mouse pancreatic islets.* J Physiol, 1998. **508 (Pt 2)**(Pt 2): p. 471-81.
120. Ren, H., et al., *Pancreatic alpha and beta cells are globally phase-locked.* Nat Commun, 2022. **13**(1): p. 3721.
121. Ravier, M.A., et al., *Loss of connexin36 channels alters beta-cell coupling, islet synchronization of glucose-induced Ca2+ and insulin oscillations, and basal insulin release.* Diabetes, 2005. **54**(6): p. 1798-807.
122. Hellman, B., et al., *Isolated mouse islets respond to glucose with an initial peak of glucagon release followed by pulses of insulin and somatostatin in antisynchrony with glucagon.* Biochem Biophys Res Commun, 2012. **417**(4): p. 1219-23.
123. Shuai, H., et al., *Fluorescent protein vectors for pancreatic islet cell identification in live-cell imaging.* Pflugers Arch, 2016. **468**(10): p. 1765-77.
124. Vergari, E., et al., *Insulin inhibits glucagon release by SGLT2-induced stimulation of somatostatin secretion.* Nat Commun, 2019. **10**(1): p. 139.
125. Kothegala, L., et al., *Somatostatin Containing delta-Cell Number Is Reduced in Type-2 Diabetes.* Int J Mol Sci, 2023. **24**(4).
126. Omar-Hmeadi, M., et al., *Paracrine control of alpha-cell glucagon exocytosis is compromised in human type-2 diabetes.* Nat Commun, 2020. **11**(1): p. 1896.

Acta Universitatis Upsaliensis

Digital Comprehensive Summaries of Uppsala Dissertations from the Faculty of Medicine 2023

Editor: The Dean of the Faculty of Medicine

A doctoral dissertation from the Faculty of Medicine, Uppsala University, is usually a summary of a number of papers. A few copies of the complete dissertation are kept at major Swedish research libraries, while the summary alone is distributed internationally through the series Digital Comprehensive Summaries of Uppsala Dissertations from the Faculty of Medicine. (Prior to January, 2005, the series was published under the title "Comprehensive Summaries of Uppsala Dissertations from the Faculty of Medicine".)

Distribution: publications.uu.se
urn:nbn:se:uu:diva-523019

ACTA UNIVERSITATIS
UPSALIENSIS
2024